Toward Efficient Drug Delivery through Suitably Prepared Metal–Organic Frameworks: A First-Principles Study

ARTICLE *in* THE JOURNAL OF PHYSICAL CHEMISTRY C · APRIL 2014

Impact Factor: 4.77 · DOI: 10.1021/jp410282m

6 AUTHORS, INCLUDING:

Emmanuel N Koukaras
Foundation for Research and Technology - Hel…
55 PUBLICATIONS **257** CITATIONS
SEE PROFILE

Pantelis N Trikalitis
University of Crete
71 PUBLICATIONS **1,884** CITATIONS
SEE PROFILE

Dimitrios N Bikiaris
Aristotle University of Thessaloniki
298 PUBLICATIONS **7,023** CITATIONS
SEE PROFILE

Aristides Zdetsis
University of Patras
125 PUBLICATIONS **1,621** CITATIONS
SEE PROFILE

THE JOURNAL OF PHYSICAL CHEMISTRY C

Article

pubs.acs.org/JPCC

Toward Efficient Drug Delivery through Suitably Prepared Metal–Organic Frameworks: A First-Principles Study

Emmanuel N. Koukaras,[†,‡] Tamsyn Montagnon,[§] Pantelis Trikalitis,[§] Dimitrios Bikiaris,[∥] Aristides D. Zdetsis,*[,†,⊥] and George E. Froudakis*[,§]

[†]Molecular Engineering Laboratory, Department of Physics, University of Patras, Patras GR-26500, Greece

[‡]Institute of Chemical Engineering Sciences, Foundation for Research & Technology Hellas (FORTH/ICE-HT), Stadiou Str. Platani, Patras 26504 Greece

[§]Department of Chemistry, University of Crete, Vasilika Vouton, Iraklion, 71003 Crete, Greece

[∥]Laboratory of Organic Chemical Technology, Department of Chemistry, Aristotle University of Thessaloniki, 541 24 Thessaloniki, Greece

[⊥]Institute of Electronic Structure and Laser, Foundation for Research & Technology Hellas, Vassilika Vouton, P.O. Box 1385, Heraklion, Crete GR-71110, Greece

ABSTRACT: With the goal in mind of developing new and much-improved drug delivery regimes for the important anticancer agent, tamoxifen; the interactions of tamoxifen with strategically modified organic linkers from IRMOFs-14 and -16 (nontoxic, high-loading, nanomaterials belonging to the metal–organic framework family) have been investigated and elucidated by means of spin-component scaled second-order Møller–Plesset perturbation theory (SCS(MI)-MP2) and density functional theory. The strategic replacement of a hydrogen atom with a hydroxyl moiety in the organic linker of IRMOF-14 and IRMOF-16 was critical for gaining key acid–base and hydrogen-bond interaction sites. The magnitudes of the maximum interaction energies with tamoxifen were found to be 16.16 kcal/mol for the modified IRMOF-14 and 18.32 kcal/mol for the modified IRMOF-16. Secondary $\pi-\pi$ type interactions of tamoxifen with the modified IRMOF-16 have also been identified, the strongest of which has an energy of between 3.0 and 5.3 kcal/mol. The type and magnitude of these combined noncovalent interactions affords appreciable multipoint binding without overbinding as is desirable for such drug delivery systems.

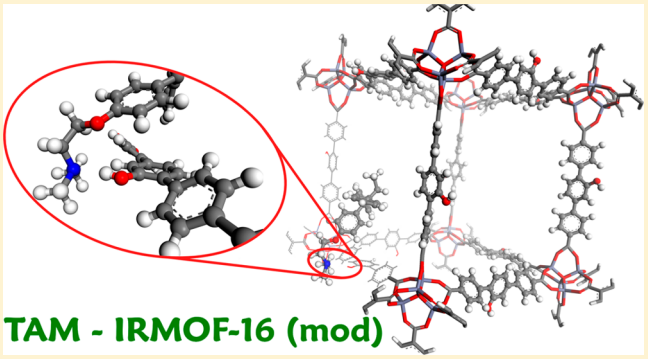

1. INTRODUCTION

If drug discovery were simply a matter of finding and synthesizing highly potent and selective molecules, there would be many more successful drugs available to treat patients-in-need by now. The dual thorns of appropriate degrees of bioavailability and in vivo drug metabolism have caused many active agents to fail in becoming drugs or have severely limited the usefulness of existing key drugs. Recently, research attention has been drawn to the idea that nanomaterials, used as novel drug delivery mechanisms, might offer interesting new solutions to these complicating issues.[1] The potential advantages of this approach include the possibility of tailoring the materials to achieve delivery site specificity and assistance in achieving long-term sustained drug release at low dosages. There is a strict set of criteria, including nontoxicity and consistent and controlled release of the drug, which must be met by any new nanomaterial drug delivery candidate. Many proposed agents of diverse structure (from biocompatible dendritic macromolecules to inorganic porous solids[2,3]) have failed for one or other of these reasons; however, it has recently been shown that hybrid metal–organic frameworks (MOFs) offer exciting potential in this therapeutic field by virtue of their low toxicity, high payloads, and controlled drug release.[4−7] MOFs are a novel family of hybrid inorganic–organic nanoporous materials.[8] The three-dimensional periodic structure of MOFs consists of inorganic secondary building units, which are linked via organic ligands. MOFs have demonstrated regular tunable porosity with high loading capacities; furthermore, the organic linker is also highly tunable making it possible to adjust the interaction with specific species (drugs). The physical characteristics of the MOFs are also highly adaptable and well-suited to the role of drug delivery agent, for example, simultaneous hydrophilic and hydrophobic character can be engineered to suit the aqueous environment of the body alongside those of a lipophilic drug candidate.

Received: October 17, 2013
Revised: March 21, 2014
Published: March 21, 2014

It was with these advantages in mind that we sought to study the potential use of MOFs as an improved drug delivery system for the important anticancer agent tamoxifen (TAM). Tamoxifen, an antagonist of the estrogen receptor in breast tissue, has been shown not only to treat very successfully certain types of breast cancer, but to deliver long-term prophylaxis in certain vulnerable patients. For long-term drug use to be successful, the drug in question must be used at as low dosages as possible and steady-state concentrations of the drug must be easy to attain and maintain. For these reasons, we opted to perform an extensive study of the binding of tamoxifen in suitable functionalized MOFs. Accordingly, we have strategically modified the organic linkers of IRMOF-14 and IRMOF-16 by inserting an acidic, aromatic hydroxyl group in order to introduce an active binding site and in particular to induce acid−base and hydrogen-bond interactions with the $-N(CH_3)_2$ group and the oxygen atom of TAM, respectively.[9−11] Although the interaction between $-N(CH_3)_2$ and aromatic −OH groups can be considered also as a hydrogen type bond, it is better to be described as an acid−base interaction. This is consistent with the amount of energy associated with this interaction, which was found to be significantly increased compared to those of typical hydrogen bonds.[12] Our target was to define significant multipoint binding of such a value that the drug would be well-absorbed by the MOF and transported to the site of interaction but that also was not so strong (what we have termed as overbinding) as to prevent the desired controlled release of the drug from the MOF. Between the two MOFs under study herein, the modified IRMOF-16 exhibited increased binding with tamoxifen (without overbinding).

2. DETAILS OF THE CALCULATIONS

All-electron calculations were performed within the framework of density functional theory (DFT) and the generalized gradient approximation (GGA) as well as calculations employing the empirically corrected spin-component scaled second-order Møller−Plesset perturbation theory (SCS(MI)-MP2)[13,14] in real space. The interaction energies of the tamoxifen molecule with the organic linkers of the modified IRMOF-14 and modified IRMOF-16 were computed by performing a potential energy surface (PES) scan with respect to various distances and orientations. The organic linkers were kept rigid at their respective optimum geometries. No constraints were imposed on TAM other than fixing the position of the nitrogen atom relative to the hydroxyl group of the organic linker to make the scan feasible. Initially, all of the geometry optimizations were performed in the framework of DFT employing the gradient corrected PBE exchange−correlation functional[15] using the Ahlrichs method[16] in Cartesian space without imposing symmetry constraints (C1). Coarse scan meshes and basis sets for all sites and approaches were used until the maximum interaction site was located. After locating the maximum interaction region, the calculations were refined and the high quality triple-ζ def2-TZVP[17] basis set was employed. For the final stage of the study, we performed ab initio calculations using spin-component scaled second-order Møller−Plesset perturbation theory (SCS(MI)-MP2), with the same high quality basis set. It has been shown[18,19] that the SCS-MP2 method with the scaling parameters originally proposed by Grimme[13] accurately predicts interaction energies for π-stacked systems; however, it underestimates the values for hydrogen-bonded systems. The quality of the results obtained by SCS(MI)-MP2 for intra- and intermolecular interaction has been shown for a wide range of systems[14,20] to be comparable to methods of much higher computational cost such as coupled cluster methods (CCSD(T)) for both hydrogen-bonded as well as dispersion type interactions. Since we anticipated the existence of both types of interactions we decided that our best choice for accurate results for systems of these sizes (taking into account computational cost) would be SCS(MI)-MP2. The optimized scaling parameters that we used are $c_{OS} = 0.17$ and $c_{SS} = 1.75$.[14] The initial geometries and molecular coordination data used in this stage of the study were taken from the results of our DFT calculations in the previous stage. At every step, we have calculated and removed the basis set superposition errors (BSSE) using the counterpoise (CP) correction method. Tight convergence criteria were enforced on the SCF energy (10^{-7} au), the one electron density (rms of the density matrix up to 10^{-7}), and the norm of the Cartesian gradient (10^{-4} au). That the correct electronic configuration has been obtained was confirmed by performing multiple calculations on different fixed spin states (singlet, triplet, etc.). All calculations were performed using the TURBOMOLE program package.[21] The calculations for the characterization of the interaction type were performed with the NCI plot code of Yang's group.[22,23]

3. RESULTS AND DISCUSSION

The organic linker of IRMOF-14, pyrene-2,7-dicarboxylate (PDC), and of IRMOF-16, *p*-terphenyl-4,4′-dicarboxylate (TPDC), were strategically modified leading to 4-pyrenol-2,7-dicarboxylate (hPDC) and 3,6-diphenylphenol-4,4′-dicarboxylate (hTPDC), respectively. The structures of hPDC and hTPDC are shown in Figure 1b and c, respectively), along with

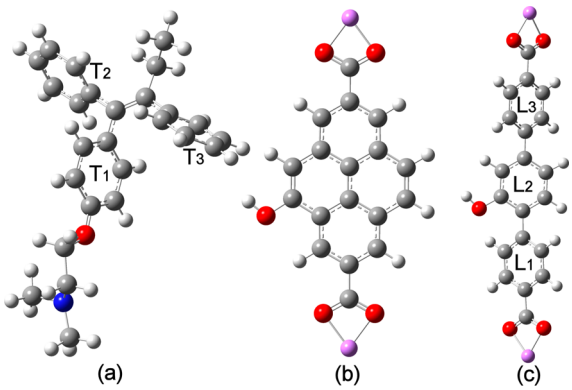

Figure 1. Key molecules from the study: (a) tamoxifen (TAM); (b,c) the organic linkers dilithium 4-pyrenol-2,7-dicarboxylate (hPDC) of the modified IRMOF-14 and dilithium 3,6-diphenylphenol-4,4′-dicarboxylate (hTPDC) of the modified IRMOF-16, respectively. The rings of TAM have been denoted T_1, T_2, and T_3 and, likewise, the rings of hTPDC with L_1, L_2, and L_3. Carbon, nitrogen, hydrogen, oxygen, and lithium atoms correspond to gray, blue, white, red, and purple, respectively. (The structures are not drawn to the same scale; reduction in scale is from left to right.).

that of tamoxifen (a). In order to reduce the computational cost, the carboxylate groups of hPDC and hTPDC were saturated with Li^+ cations. This truncated model system provides a good representation[24−27] of the effect of the inorganic part on the organic linkers and is not expected to alter the results in any significant way.

dx.doi.org/10.1021/jp410282m | J. Phys. Chem. C 2014, 118, 8885−8890

At each point of the scan, for a selected (constant) distance, the structures of both tamoxifen and of the organic linkers were allowed to relax and optimize. The interaction energy, E_{int}, at each point was determined by the usual relationship:

$$E_{int} = E_{linker+tamoxifen} - (E_{linker} + E_{tamoxifen})$$

in which the BSSE corrections, as was mentioned earlier, have been included using the counterpoise (CP) method.

The hPDC ligand has a length that equates to a window size in the final structure of the modified IRMOF-14 that is suitable for the absorption of tamoxifen. Yaghi et al.[8] provide dimensions of absorbed molecules able to diffuse through the pore apertures. For IRMOF-14 the free diameter is calculated at 13.8 Å. A crude ellipsoid model of TAM has principle axes lengths of 14.6, 11.3, and 4.2 Å, which allows for easy diffusion through the apertures. Our results show that the introduction of the aromatic hydroxyl group into the structure of hPDC provided an active site at which TAM interacts noncovalently (NC). The maximum interaction was found to be between the nitrogen atom of TAM and the hydrogen atom of the hydroxyl group of hPDC. This noncovalent bond length $N_{TAM}\cdots HO_{hPDC}$ was found to be 1.8 Å. A second and much weaker interaction between $O_{TAM}\cdots HO_{hPDC}$ has also been identified with a bond length of 2.8 Å at the overall maximum interaction configuration. The magnitude of the maximum overall interaction was calculated to be 16.16 kcal/mol. It is proposed that the existence of the nearby oxygen atom in the TAM molecule may lead to an additional hydrogen-bond interaction that contributes and increases the overall interaction energy. The main contribution to the interaction energy is an acid–base interaction between the $-N(CH_3)_2$ of TAM and the acidic −OH of the organic linker (see section 3.1). To rule out any possibility of an effect introduced by the dilithium termination the calculation was repeated using the hPDC structure terminated with the full inorganic cluster (Figure 2). Essentially the same (+0.2 kcal/mol) interaction energy was found as had been previously calculated.

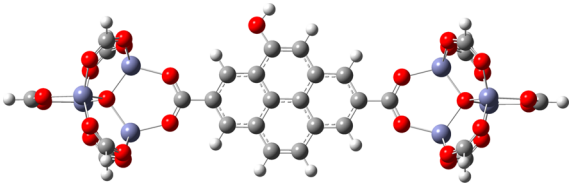

Figure 2. Organic linker of the modified IRMOF-14 terminated with the complete inorganic clusters. Carbon, nitrogen, hydrogen, oxygen, and lithium atoms correspond to gray, blue, white, red, and purple, respectively.

Having completed this first stage of the study, we choose to move on and investigate a change in the organic linker with the idea of improving the MOF characteristics and binding potential. The potential of the MOF to act as a drug delivery vehicle would be improved by widening the window through which tamoxifen molecules enter the main body of the nanopourous material. In addition, an organic linker with more flexible phenyl rings may also promote some degree of $\pi-\pi$ interaction between the electron-rich TAM phenyl groups and the electron deficient (due to −COOH substitution) phenyl groups of the linker. With this reasoning in mind, we chose to investigate a modified IRMOF-16 organic linker, namely, hTPDC (Figure 1c).

The longer length of hTPDC permits for slightly easier absorption of TAM into the MOF crystal without the window becoming too large to lose (volumetric) efficiency. For IRMOF-16 the free diameter is calculated[8] at 19.1 Å. This size is large compared to the dimensions of TAM even if an impact of the functionalization on the pore dimensions is considered. As in the case of hPDC linker, we choose to add one aromatic −OH group in the central ring in order to avoid unfavorable steric effects. In this way TAM will anchor on the aromatic −OH group at a distance from the inorganic cluster as well as from the electron withdrawing carboxyl groups. Furthermore, the nonplanar relative orientation of the phenyl groups hinders charge transfer between them, buffering the electron density of the central phenyl group. These factors ensure high acidity for the aromatic hydroxyl group, and in this way, an enhanced TAM–MOF interaction is anticipated. A straightforward methodology for the synthesis of similar, hydroxyl functionalized carboxylate-based linkers has been reported recently,[28] and therefore, with proper modifications the proposed ligands could be experimentally synthesized. As we show in the following section, the maximum interaction was found to be between the nitrogen of TAM and the hydrogen of the hydroxyl group of hTPDC. Specifically, at the maximum interaction coordination the $N_{TAM}\cdots HO_{hTPDC}$ bond length is 1.94 Å, while the O–Ĥ···N angle is 154.6°. The magnitude of the maximum interaction energy between TAM and hTPDC was found to be 18.32 kcal/mol, which is higher compared to that of hPDC linker. We restricted the potential energy surface scan to this maximum interaction region, the results of which are shown in Figure 3.

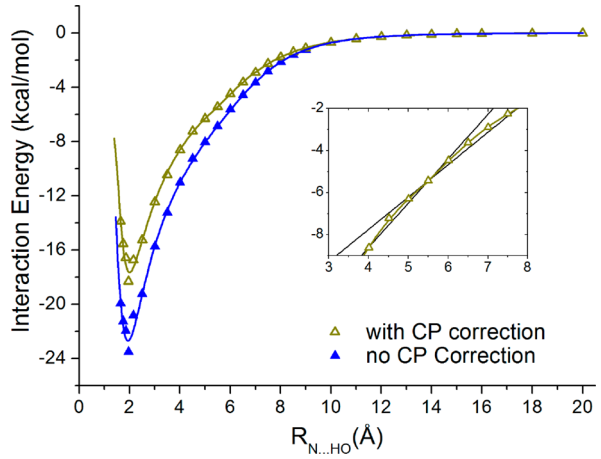

Figure 3. Interaction energy at the maximum interaction configuration of TAM with dilithium 3,6-diphenylphenol-4,4′-dicarboxylate (hTPDC) (organic linker of the modified IRMOF-16).

The interaction energy of TAM with the original, unmodified, TPDC structure was calculated at 8.2 kcal mol^{-1} at the SCS(MI)-MP2 level of theory. The introduction of the hydroxyl unit in the TPDC structure results in an increase of interaction energy by a factor of 2.2 to 18.3 kcal mol^{-1}. Values in this vicinity are deemed suitable for drug delivery with delayed release, as reported [ref 7 and references therein] by Babarao and Jiang between certain drugs and members of the MIL family of MOFs, such as that of MIL-101 and ibuprofen (at 17.48 kcal mol^{-1}). Another well suited example is the work of Horcajada et al. [ref 6 and references therein] on the adsorption of ibuprofen by MIL-53(Fe). In that case the main

dx.doi.org/10.1021/jp410282m | J. Phys. Chem. C 2014, 118, 8885–8890

interaction was hydrogen-bonding type found between the carboxylic group of ibuprofen and the hydroxyl group at the surface of the matrix. Other interactions included van der Waals and/or CH−π type between methyl groups of ibuprofen and the benzene ring of the terephthalic linker of MIL53(Fe). They report the interaction energy at 13.6 kcal mol^{-1}. The higher interaction energies in the case of the modified IRMOF-16 and TAM can be attributed to a simultaneous combination of the contributing terms; specifically the $N_{TAM}\cdots HO_{hPDC}$, $O_{TAM}\cdots HO_{hPDC}$, and $\pi-\pi$ interactions as well as the high acidity of the aromatic hydroxyl group. Of course, small discrepancies are also expected to arise when different computational methodologies are applied for the treatment of dispersion forces.

3.1. Reduced Electron Density Gradient. In addition to examining the bond length, bond angles, and interaction energies, we have further investigated the interaction in this region by examining the reduced electron density gradient. The reduced electron density gradient s is defined[23] as

$$s = \frac{1}{2(3\pi^2)^{1/3}}\frac{|\nabla\rho|}{\rho^{4/3}} \quad (1)$$

where ρ is the electron density obtained in this case from DFT calculations employing the PBE functional and using the def2-TZVP basis set. In Figure 4, the reduced density gradient has been plotted as a function of ρ multiplied by the sign of the λ_2 eigenvalue of the electron density Hessian matrix, $\text{sin}(\lambda_2)\rho$. In this plot, the steep peaks in the low-density low-gradient regions indicate noncovalent interactions (NCI). Furthermore, bonding interactions are identified by a negative value of λ_2. The peak (of signed ρ) at −0.033 au (denoted as "1" in Figure 4) indicates an acid−base interaction in the region between the nitrogen atom of TAM and the hydrogen atom of the hydroxyl unit of hTPDC. Similarly, the peak near −0.004 au (denoted as "2" in Figure 4) may support the idea that an additional hydrogen-bond interaction exists between the oxygen atom of TAM and the hydrogen atom of the hydroxyl group of hTPDC.

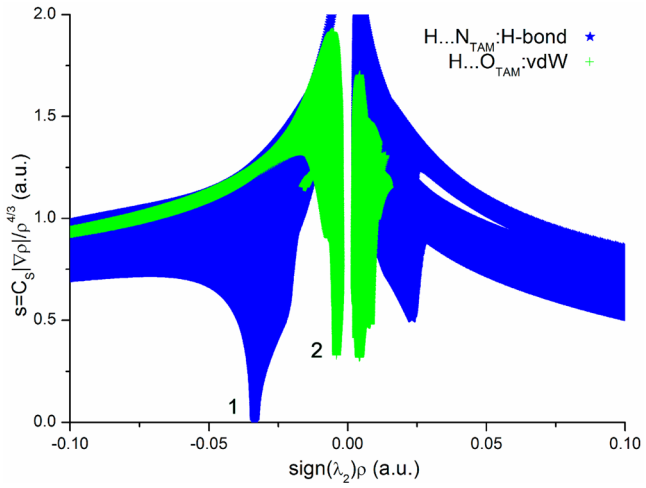

Figure 4. Reduced density gradient s versus the electron density ρ multiplied by the sine of the second Hessian eigenvalue. The data corresponds to the region between (a) the nitrogen atom of TAM and the hydrogen of the hydroxyl moiety of hTPDC, denoted by the blue stars, and (b) the oxygen atom of TAM and the hydrogen of the hydroxyl moiety of hTPDC, denoted by the green crosses. Data was obtained from PBE/def2-TZVP density and gradient values on very dense 0.0125 au (a) cuboid and (b) radial grids.

The sampling of the regions of interest for the calculations of the reduced density gradient was performed using very dense 0.0125 au cuboid ($N_{TAM}\cdots HO_{hTPDC}$) and radial ($O_{TAM}\cdots HO_{hTPDC}$) grids.

Although it would be of interest, we were unable to formulate a reliable method to attribute the percentage that each NC bond, namely, the $N_{TAM}\cdots HO_{hTPDC}$ and $O_{TAM}\cdots HO_{hTPDC}$ interactions, contributes to the overall interaction energy. However, on the basis of the NCI diagrams we can conclude that both interactions are attractive, while the magnitude of the $N_{TAM}\cdots HO_{hTPDC}$ is much stronger than that of the $O_{TAM}\cdots HO_{hTPDC}$.

We have generated a low-gradient isosurface (s = 0.5 au) constrained to low densities, which is displayed in Figure 5. The color mapping corresponds to the values of $\text{sin}(\lambda_2)\rho$. The blue color of the isosurface in Figure 5 indicates a strong attractive interaction. The data for the $N_{TAM}\cdots HO_{hTPDC}$ interaction in both Figures 4 and 5 was obtained from the PBE/def2-TZVP electron density, which is appropriate for such calculations,[23] and gradient values on a very dense (0.0125 au) cuboid grid. A similar region, albeit of weak intensity, was found for the $O_{TAM}\cdots HO_{hTPDC}$ interaction, shown in Figure 5 with green color, this represents the secondary and weaker hydrogen-bond interaction.

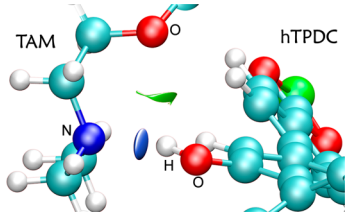

Figure 5. Partial view of the structures of TAM (left) and the hTPDC organic linker (right). The reduced density gradient isosurface (s = 0.5 au) for the region between the N_{TAM} and the HO_{hTPDC}. The blue color of the surface corresponds to a negative $\text{sin}(\lambda_2)\rho$ and indicates a strong and attractive noncovalent, acid−base interaction.

3.2. $\pi-\pi$ Interactions. An advantage of hTPDC is that it consists of freely rotating phenyl rings, which are accessible by the phenyl-rings of tamoxifen in coordinations that facilitate the formation of $\pi-\pi$ interactions. In Figure 1 we denoted the three rings of tamoxifen with T_1, T_2, and T_3 and the rings of hTPDC as L_1, L_2 (phenol), and L_3. The description of $\pi-\pi$ interactions can be rather challenging due to their small magnitude (up to 5−6 kcal/mol).[20] In Figure 6, benzene and phenol have been used as a model system to denote the most favorable $\pi-\pi$ stacking type configurations. These are parallel displaced (PD, or sandwich for R = 0; Figure 6a); perpendicular

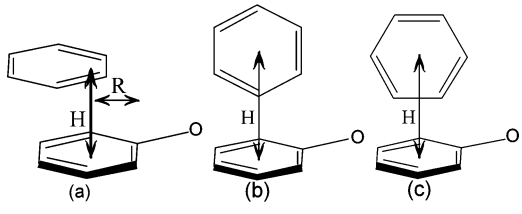

Figure 6. Three possible types of stacking between aromatic rings to be found in the structures similar to those under study. Specifically, (a) parallel displaced (PD) or sandwich (S, for R = 0); (b) T-shaped; and (c) edge-face (EF) T-shaped $\pi-\pi$ ring interaction coordinations.

dx.doi.org/10.1021/jp410282m | J. Phys. Chem. C 2014, 118, 8885−8890

T-shaped (Figure 6b); and edge-face (EF) T-shaped (Figure 6c). The distance between the center of mass of the rings is denoted by *H*, while the parallel displacement is denoted by *R*. As the magnitude of $\pi-\pi$ interactions is small, their importance in these systems stems from their contribution to an organized multipoint binding of drug to MOF (analogous to classical drug-receptor binding models).

The optimized parallel displaced π-stacked configuration of TAM with hTPDC, which exhibits the strongest $\pi-\pi$ type interaction, is shown in Figure 7. The interaction energy in this

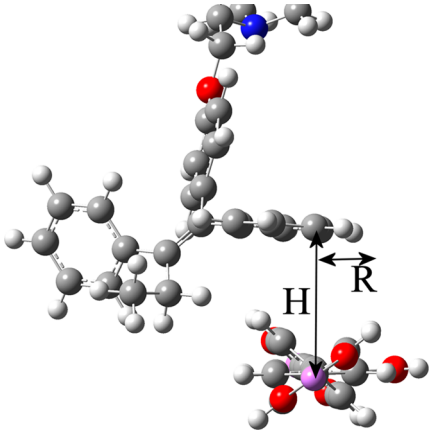

Figure 7. Optimized sandwich type π-stacked coordination between the T_2 and L_2 rings of TAM and hTPDC, respectively. The distance between the center of the rings is denoted by *H* and the parallel displacement by *R*.

case was found to be 5.3 kcal/mol. The parameters of this coordination are given in Table 1, along with the parameters

Table 1. Interaction Energy for π-Stacked Configurations between Rings of TAM and hTPDC[a]

stacking	ring 1	ring 2	*H* (Å)	*R* (Å)	E_{int} (kcal/mol)
PD	L_2	T_2	4.5	0.8	5.3
T-shaped	L_2	T_2	5.3		3.3
EF T-shaped	L_2	T_2	5.4		3.1
PD[b]	L_2	T_3	4.2	2.9	4.6

[a]We note the (ideal) stacking type, the rings involved, and the defining parameters (H and R) of the coordination. The configurations listed are optimal cases isolated from hydrogen-bond contributions. [b]In the last case listed, the tilt angle between rings 1 and 2 is 11.1°.

and values for the next three strongest interactions (of this and other types) found. The cases listed in Table 1 correspond to optimal π-stacked configurations with acceptable isolation from hydrogen-bond contributions (the distance of the nitrogen and oxygen atoms of TAM from the hydroxyl unit of hTPDC is well above 10 Å in every case). The longer length and greater flexibility of the hTPDC linker compared to the hPDC linker has permitted the formation of a secondary $\pi-\pi$ interaction (Figure 7) that contributes positively to the overall attractive interaction between tamoxifen and MOF.

At the overall maximum interaction configuration there is a component of the interaction energy that stems from π-stacking between the rings T_1 and L_2 of TAM and hPDC, respectively. The narrow form of hTPDC permits for the existence of these types of coordination; however, spatial restrictions still apply and lead to nonoptimial π-stacking configuration. More specifically, at the maximum interaction configuration the distance between the rings is H = 4.3 Å with a parallel displacement of R = 1.3 Å and a tilt angle of 33.0°.

The existence of $\pi-\pi$ interactions has a noticeable effect on the form of the interaction energy curve given in Figure 3. The main effect is the broadening of the potential well. Because of the extensive size of tamoxifen, as the distance of the nitrogen atom of tamoxifen from the hydroxyl moiety increases, a π-stacked configuration forms between the T_2 and L_3 rings, which persists up to a $N_{TAM}\cdots HO_{hTPDC}$ distance of 5.5 Å. The increase in the parallel displacement between the T_2 and L_3 rings (as the $N_{TAM}\cdots HO_{hTPDC}$ distance increases) results in the decrease of the $\pi-\pi$ contribution to the interaction energy. The inset of Figure 3 shows a sudden change in the slope of the interaction energy curve at this point, beyond which the interaction energy decreases at a slightly greater rate. This coincides to a coordination at which the two rings are out of scope.

4. CONCLUSIONS

The study presented herein has succeeded in identifying, strategically modifying, and then studying in detail, using a variety of different, but complementary, computational tools; the nanomaterial/drug interactions for two new drug delivery candidates belonging to the MOF nanomaterial family. These MOFs (IRMOF-14 and IRMOF-16), which offer a slew of potential advantages within the general context of improved tamoxifen therapy regimes (vide infra), were also selected for the more specific reason that they held the potential to participate in both key hydrogen-bonding and in $\pi-\pi$ interactions with the tamoxifen. Following the strategic modification of the selected MOFs, highly desirable multipoint, noncovalent, binding with tamoxifen was shown to have been attained. The maximum interaction energies of 16.16 kcal/mol for IRMOF-14 and 18.32 kcal/mol for IRMOF-16 represent binding energies that are adequate for the drug's absorption and delivery without its strength prohibiting the timely release of the drug within the body (binding without overbinding). Furthermore, the study revealed that between tamoxifen and OH-IRMOF-16 both acid–base and hydrogen-bond interactions exists, coupled with weaker, but not insignificant, $\pi-\pi$ interactions.

In summary, this study has shown that MOFs could offer a great and highly tunable drug delivery solution to the conundrum of how to improve the in vivo characteristics and overall efficacy of tamoxifen and, potentially, of many other important drugs as well.

AUTHOR INFORMATION

Corresponding Authors

*(G.E.F.) E-mail: frudakis@chemistry.uoc.gr.

*(A.D.Z.) E-mail: zdetsis@upatras.gr.

Notes

The authors declare no competing financial interest.

ACKNOWLEDGMENTS

A.D.Z. acknowledges financial support from the EU-project ENSEMBLE (grant no. 213669).

REFERENCES

(1) Hughes, G. A. Nanostructure-Mediated Drug Delivery. *Nanomed.: Nanotechnol., Biol. Med.* **2005**, *1*, 22–30.

(2) Dhivanand, P.; Sprockel, O. L. A Controlled Porosity Drug Delivery System. *Int. J. Pharm.* **1998**, *167*, 83−96.
(3) Rivera, A.; Farías, T. Clinoptilolite−Surfactant Composites as Drug Support: A New Potential Application. *Microporous Mesoporous Mater.* **2005**, *80*, 337−346.
(4) Horcajada, P.; Chalati, T.; Serre, C.; Gillet, B.; Sebrie, C.; Baati, T.; Eubank, J. F.; Heurtaux, D.; Clayette, P.; Kreuz, C.; et al. Porous Metal−Organic-Framework Nanoscale Carriers as a Potential Platform for Drug Delivery and Imaging. *Nat. Mater.* **2010**, *9*, 172−178.
(5) Horcajada, P.; Serre, C.; Vallet-Reg, M.; Sebban, M.; Taulelle, F.; Férey, G. Metal−Organic Frameworks as Efficient Materials for Drug Delivery. *Angew. Chem., Int. Ed.* **2006**, *45*, 5974−5978.
(6) Horcajada, P.; Serre, C.; Maurin, G.; Ramsahye, N. A.; Balas, F.; Vallet-Regí, M.; Sebban, M.; Taulelle, F.; Férey, G. Flexible Porous Metal−Organic Frameworks for a Controlled Drug Delivery. *J. Am. Chem. Soc.* **2008**, *130*, 6774−6780.
(7) Babarao, R.; Jiang, J. Unraveling the Energetics and Dynamics of Ibuprofen in Mesoporous Metal−Organic Frameworks. *J. Phys. Chem. C* **2009**, *113*, 18287−18291.
(8) Eddaoudi, M.; Kim, J.; Rosi, N.; Vodak, D.; Wachter, J.; O'Keeffe, M.; Yaghi, O. M. Systematic Design of Pore Size and Functionality in Isoreticular MOFs and Their Application in Methane Storage. *Science* **2002**, *295*, 469−472.
(9) Koukaras, E. N.; Froudakis, G. E.; Zdetsis, A. D. Theoretical Study of Amino Acid Interaction with Metal Organic Frameworks. *J. Phys. Chem. Lett.* **2011**, *2*, 272−275.
(10) Klontzas, E.; Mavrandonakis, A.; Tylianakis, E.; Froudakis, G. E. Improving Hydrogen Storage Capacity of MOF by Functionalization of the Organic Linker with Lithium Atoms. *Nano Lett.* **2008**, *8*, 1572−1576.
(11) Mulfort, K.; Farha, O.; Stern, C.; Sarjeant, A.; Hupp, J. Post-Synthesis Alkoxide Formation Within Metal−Organic Framework Materials: A Strategy for Incorporating Highly Coordinatively Unsaturated Metal Ions. *J. Am. Chem. Soc.* **2009**, *131*, 3866−3868.
(12) Kogowski, G.; Scott, R. M.; Fllisko, F. Enthalpy Change of Hydrogen Bond Formation Between ortho-Substituted Phenols and Aliphatic Amines. *J. Phys. Chem.* **1980**, *84*, 2262−2265.
(13) Grimme, S. Improved Second-Order Møller−Plesset Perturbation Theory by Separate Scaling of Parallel- and Antiparallel-Spin Pair Correlation Energies. *J. Chem. Phys.* **2003**, *118*, 9095.
(14) Distasio, R. A.; Head-Gordon, M. Optimized Spin-Component Scaled Second-Order Møller−Plesset Perturbation Theory for Intermolecular Interaction Energies. *Mol. Phys.* **2007**, *105*, 1073−1083.
(15) Perdew, J. P.; Burke, K.; Ernzerhof, M. Generalized Gradient Approximation Made Simple. *Phys. Rev. Lett.* **1996**, *77*, 3865−3868.
(16) Arnim, M. V.; Ahlrichs, R. Geometry Optimization in Generalized Natural Internal Coordinates. *J. Chem. Phys.* **1999**, *111*, 9183.
(17) Weigend, F.; Ahlrichs, R. Balanced Basis Sets of Split Valence, Triple Zeta Valence and Quadruple Zeta Valence Quality for H to Rn: Design and Assessment of Accuracy. *Phys. Chem. Chem. Phys.* **2005**, *7*, 3297−3305.
(18) Hohenstein, E. G.; Sherrill, C. D. Effects of Heteroatoms on Aromatic $\pi-\pi$ Interactions: Benzene−Pyridine and Pyridine Dimer. *J. Phys. Chem. A* **2009**, *113*, 878−886.
(19) Bachorz, R. A.; Bischoff, F. A.; Höfener, S.; Klopper, W.; Ottiger, P.; Leist, R.; Frey, J. A.; Leutwyler, S. Scope and Limitations of the SCS-MP2 Method for Stacking and Hydrogen Bonding Interactions. *Phys. Chem. Chem. Phys.* **2008**, *10*, 2758−2766.
(20) Řezáč, J.; Riley, K. E.; Hobza, P. S66: A Well-balanced Database of Benchmark Interaction Energies Relevant to Biomolecular Structures. *J. Chem. Theory Comput.* **2011**, *7*, 2427−2438.
(21) *TURBOMOLE* (version 5.6); Universitat Karlsruhe: Karlsruhe, Germany, 2000.
(22) Contreras-García, J.; Johnson, E. R.; Keinan, S.; Chaudret, R.; Piquemal, J.-P.; Beratan, D. N.; Yang, W. NCIPLOT: A Program for Plotting Noncovalent Interaction Regions. *J. Chem. Theory Comput.* **2011**, *7*, 625−632.
(23) Johnson, E. R.; Keinan, S.; Mori-Sánchez, P.; Contreras-Garcıá, J.; Cohen, A. J.; Yang, W. Revealing Noncovalent Interactions. *J. Am. Chem. Soc.* **2010**, *132*, 6498−6506.
(24) Hubner, O.; Gloss, A.; Fichtner, M.; Klopper, W. On the Interaction of Dihydrogen with Aromatic Systems. *J. Phys. Chem. A* **2004**, *108*, 3019−3023.
(25) Sagara, T.; Klassen, J.; Ortony, J.; Ganz, E. Binding Energies of Hydrogen Molecules to Isoreticular Metal−Organic Framework Materials. *J. Chem. Phys.* **2005**, *123*, 014701.
(26) Mavrandonakis, A.; Tylianakis, E.; Stubos, A. K.; Froudakis, G. E. Why Li Doping in MOFs Enhances H_2 Storage Capacity? A Multiscale Theoretical Study. *J. Phys. Chem. C* **2008**, *112*, 7290−7294.
(27) Klontzas, E.; Mavrandonakis, A.; Froudakis, G. E.; Carissan, Y.; Klopper, W. Molecular Hydrogen Interaction with IRMOF-1: A Multiscale Theoretical Study. *J. Phys. Chem. C* **2007**, *111*, 13635−13640.
(28) Spanopoulos, I.; Xydias, P.; Malliakas, C. D.; Trikalitis, P. N. A Straight Forward Route for the Development of Metal−Organic Frameworks Functionalized with Aromatic −OH Groups: Synthesis, Characterization, and Gas (N_2, Ar, H_2, CO_2, CH_4, NH_3) Sorption Properties. *Inorg. Chem.* **2013**, *52*, 855−862.

NOTE ADDED AFTER ASAP PUBLICATION

This paper was published on the Web on April 23, 2014. An additional affiliation was added for author A. D. Zdetsis, as well as adding an Acknowedgment paragraph. The corrected version was reposted on May 1, 2014.